Astronomy & Astrophysics manuscript no. main
March 14, 2023

Calculating the CMB power spectrum (or a more spicy title)

Nanna Bryne[1, 2]

[1] Institute of Theoretical Astrophysics (ITA), University of Oslo, P.O. Box 1029 Blindern, N-0315 Oslo, Norway
[2] Center for Computing in Science Education (CCSE), Dept. of Physics, University of Oslo, P.O. Box 1048 Blindern, N-0316 Oslo, Norway
e-mail: `nanna.bryne@fys.uio.no`

March 14, 2023

ABSTRACT

ABSTRACT

Key words. cosmic microwave background - large-scale structure of universe

1. Introduction

The overall purpose of this project is to produce a program that calculates the Cosmic Microwave Background (CMB) power spectrum and predict the CMB and matter fluctuations through it. We want to achieve this starting from first principles. A large part of this paper follows (Callin 2006).

We consider the concordance model of cosmology model that a Eucledean universe currently dominated by non-baryonic cold dark matter (CDM) and a cosmological constant (Λ), namely the (flat) ΛCDM model. The cosmological constant Λ is used as a moniker for dark energy (DE). (Dodelson & Schmidt 2021)

Complementary material to this paper can be found in our Github repository at `https://github.com/nannabryne/AST5220`.

2. Background cosmology

The first ingredient in the aforementioned program is a numerical framework describing the (unperturbed) background geometry. Said geometry is determined by the Friedmann-Robertson-Walker (FRW) metric and, as a starting point, a flatness assumption. However, we keep the variables associated with the curvature, the reasoning behind which will become clear shortly.

We want to describe the evolution of the Hubble parameter, conformal time and distance measures, all as functions of the logarithmic scale factor, $x = \ln a$, working as the main time variable in this paper. This is to be done with the use of the fiducial parameters ("fiducials") from (Planck Collaboration et al. 2021).

The implementation of these functions results in a cosmological model that we can play around with. Our next task is to use observational data from (Betoule et al. 2014) to tweak the default cosmological parameters and evaluate their credibility, curvature being one of the parameters. In particular, we will use a Monte Carlo Markov Chain (MCMC) with Metropolis algorithm to explore the parameter space of our model to infer their properties and compare them with observations from supernovae.

MCMC is a popular statistical technique used in various fields besides cosmology. The Metropolis algorithm, a simple and widely used MCMC method, generates a Markov chain of samples in a data set that converge to the target distribution by iteratively accepting or rejecting proposed moves in parameter space based on a set of acceptance criteria.

2.1. Theory

The FRW line element in flat space is given by

$$\begin{aligned} ds^2 &= -c^2 \mathrm{d}t^2 + a^2(t)\delta_{ij}\mathrm{d}x^i\mathrm{d}x^j \qquad |\, \mathrm{d}\eta \equiv c\mathrm{d}t\, a^{-1}(t) \\ &= a^2(t)\left(-\mathrm{d}\eta^2 + \delta_{ij}\mathrm{d}x^i\mathrm{d}x^j\right). \end{aligned} \tag{1}$$

Before we proceed, we substitute $a \to \mathrm{e}^x$ (recall: $x = \ln a$). The cosmic time t and Hubble parameter H ($= \mathrm{d}x/\mathrm{d}t$) will be replaced by the conformal time η ($\mathrm{d}\eta = c\mathrm{e}^{-x}\mathrm{d}t$) and conformal Hubble parameter $\mathcal{H} \equiv aH$ ($= c\mathrm{d}x/\mathrm{d}\eta$). We write the Friedmann equations in terms of our preferred variables, which for the first one becomes

$$\mathcal{H}(x) = H_0\sqrt{\Omega_{\mathrm{m0}}\mathrm{e}^{-x} + \Omega_{\mathrm{r0}}\mathrm{e}^{-2x} + \Omega_{\mathrm{K0}} + \Omega_{\Lambda 0}\mathrm{e}^{2x}}, \tag{2}$$

the components of which are to be discussed shortly. The operator

$$\frac{\mathrm{d}}{\mathrm{d}x} = \frac{c}{\mathcal{H}}\frac{\mathrm{d}}{\mathrm{d}\eta} = \frac{1}{H}\frac{\mathrm{d}}{\mathrm{d}t} \tag{3}$$

proves useful, giving both the ordinary differential equation (ODE) for $\eta(x)$ and $t(x)$,

$$\frac{\mathrm{d}\eta}{\mathrm{d}x} = \frac{c}{\mathcal{H}(x)}\,; \qquad \eta(x_{\mathrm{init}}) = \eta_{\mathrm{init}}, \tag{4a}$$

$$\frac{\mathrm{d}t}{\mathrm{d}x} = \frac{1}{H} = \frac{\mathrm{e}^x}{\mathcal{H}(x)}\,; \qquad t(x_{\mathrm{init}}) = t_{\mathrm{init}}, \tag{4b}$$

where, in theory, $x_{\mathrm{init}} \to -\infty$ and the initial conditions $t_{\mathrm{init}}, \eta_{\mathrm{init}} \to 0$. However, we can solve Eq. (4) analytically in the very early universe and in Sec. 2.1.2 we present these expressions (Eq. (11)).

Finally, the cosmological redshift $z = \mathrm{e}^{-x} - 1$ will be used as an auxiliary time variable.

2.1.1. Density parameters

We assume the constituents of the universe to be cold dark matter (CDM (c)), baryons (b), photons (γ), neutrinos (ν) and a cosmological constant (Λ). We may regard the curvature (K) as a constituent as well. The evolution of the density parameter Ω_s associated with cosmological component $s \in \{c, b, \gamma, \nu, \Lambda, K\}$ can be described in terms of our preferred variables as

$$\Omega_s(x) = \frac{\Omega_{s0}}{e^{(1+3w_s)x}\mathcal{H}^2(x)/H_0^2}\,; \quad \Omega_{s0} \equiv \Omega_s(x = x_0), \tag{5}$$

where H_0 is the Hubble constant, $x_0 = \ln a_0 = 0$ means *today* and the *equation of state* parameter w_s is a constant intrinsic to the species s. As a notational relief, we introduce the parameters associated with total matter (m) and relativistic particles (r) such that $w_m = 0$, $w_r = 1/3$, $w_\Lambda = -1$ and $w_K = -1/3$, and

$$\Omega_m = \Omega_c + \Omega_b \quad \text{and} \quad \Omega_r = \Omega_\gamma + \Omega_\nu. \tag{6}$$

Eq. (5) requires the current values of the density parameters. The observed CMB temperature today T_{CMB0} gives today's photon density

$$\Omega_{\gamma 0} = 2\frac{\pi^2}{30}\frac{(k_b T_{CMB0})^4}{\hbar^3 c^5}\frac{8\pi G}{3H_0^2}, \tag{7}$$

and followingly the neutrino density today

$$\Omega_{\nu 0} = N_{eff} \cdot \frac{7}{8}\left(\frac{4}{11}\right)^{4/3}\Omega_{\gamma 0}, \tag{8}$$

N_{eff} being the effective number of massless neutrinos. From the Friedmann equations, the total density adds up to one, so we can determine the cosmological constant through $\Omega_{\Lambda 0} = 1 - \sum_s \Omega_{s0}$. Together with current values for the remaining densities, we have the evolution of all the considered constituents' densities as functions of x. This allows us to pinpoint the time when the total matter and radiation densities are equal – the "radiation-matter equality" – as $\Omega_m(x = x_{eq}) = \Omega_r(x = x_{eq})$. Further, we find the time at which the universe becomes dominated by the cosmological constant as $\Omega_\Lambda(x = x_\Lambda) = \Omega_m(x = x_\Lambda)$.

2.1.2. Expansion and analytical approximations

To study the geometry of the universe, we want to know when the expansion started, i.e. when the universe started accelerating: $\mathrm{d}^2a\big/\mathrm{d}t^2$. It is trivial to show that this condition is equivalent to requiring $\mathrm{d}\mathcal{H}/\mathrm{d}x\,|_{x=x_{acc}} = 0$. In App. A we present analytical expressions for the derivatives of $\mathcal{H}(x)$ in x. Studying these expressions, we expect to see that the start of acceleration and time of matter-dark energy transition are close to each other ($x_{acc} \sim x_\Lambda$).

The first Friedmann equation can be written in the general form

$$\mathcal{H}(x) = H_0\sqrt{\sum_s \Omega_{s0}e^{-(1+3w_s)x}}, \tag{9}$$

where sum over s is a sum over the constituents in the universe ($s \in \{m, r, \Lambda, K\}$). In an era where e.g. radiation dominates heavily ($\Omega_r(x) \to 1$), the parameter resembles that of a universe with $\Omega_{r0} = 1$ and so $\mathcal{H}(x) \simeq H_0\sqrt{\Omega_{r0}e^{-2x}}$. In more general terms, the conformal Hubble factor during an era dominated by a collection of particles with the same equation of state – a species s – is approximated

$$\mathcal{H}(x) \simeq H_0\sqrt{\Omega_{s0}}e^{-\frac{x}{2}(1+3w_s)}. \tag{10}$$

If for said species we have $\Omega_s(x) \simeq 1$, we get $\Omega_{s'}(x) \ll 1$ for the others, and we expect this to be very close to equality.

In the very early universe, only relativistic particles were present. Conveniently, this gives nice expressions for the initial conditions for Eq. (4):

$$\eta_{init} = \frac{c}{\mathcal{H}(x_{init})}$$
$$t_{init} = \frac{e^{x_{init}}}{2\mathcal{H}(x_{init})} \tag{11}$$

The remaining task is then to choose a suitable $x_{init} < x_{eq}$.

2.1.3. Distance measures

Say we want to allow for the possibility of an open ($k = -1$) or closed ($k = +1$) universe, as opposed to the initial flatness ($k = 0$) assumption. In spherical coordinates, the FRW line element (Eq. (1)) is

$$ds^2 = e^{2x}\left(-\mathrm{d}\eta^2 + \frac{\mathrm{d}r^2}{1-kr^2} + r^2\mathrm{d}\theta^2 + r^2\sin^2\theta\,\mathrm{d}\phi^2\right), \tag{12}$$

and $k = -\Omega_{K0}H_0^2/c^2$. Consider a radially moving ($\mathrm{d}r < 0$; $\mathrm{d}\theta^2 = \mathrm{d}\phi^2 = 0$) photon ($ds^2 = 0$) travelling from a distance r at conformal time η to reach Earth ($r = 0$) today ($\eta = \eta_0$). Eq. (12) gives

$$\int_r^0 \frac{-\mathrm{d}r'}{\sqrt{1-kr'^2}} = \int_\eta^{\eta_0}\mathrm{d}\eta' \tag{13}$$

of which the right-hand side is the co-moving distance $\chi = \eta_0 - \eta$. We evaluate the left integral in Eq. (13) and find

$$r(\chi) = \begin{cases} \chi \cdot \frac{\sin\left(\sqrt{|\Omega_{K0}|}H_0\chi/c\right)}{\sqrt{|\Omega_{K0}|}H_0\chi/c} & \Omega_{K0} < 0 \\ \chi & \Omega_{K0} = 0\,. \\ \chi \cdot \frac{\sinh\left(\sqrt{|\Omega_{K0}|}H_0\chi/c\right)}{\sqrt{|\Omega_{K0}|}H_0\chi/c} & \Omega_{K0} > 0 \end{cases} \tag{14}$$

The angular diameter distance of an object of physical size D and angular size θ is $d_A = D/\theta$. From Eq. (12) we get $\mathrm{d}D = re^x\mathrm{d}\theta$ and so

$$d_A(x) = re^x. \tag{15}$$

The luminosity distance is $d_L = d_A e^{-2x}$, giving

$$d_L(x) = re^{-x}. \tag{16}$$

2.2. Implementation details

The code we wrote included a class in C++ representing the background. In particular, this class requires current values of the density parameters Ω_{b0}, Ω_{CDM0} and Ω_{K0}, the CMB temperature today (T_{CMB0}) and the effective neutrino number (N_{eff}). In addition, the class needs the "little" Hubble constant $h = H_0$ [100 km s^{-1} Mpc^{-1}]. The remaining density parameters are computed as elaborated in Sec. 2.1. Amongst the class methods are functions for computing $\mathcal{H}(x)$, $\mathrm{d}\mathcal{H}(x)/\mathrm{d}x$, $\mathrm{d}^2\mathcal{H}(x)\big/\mathrm{d}x^2$ and $\Omega_{s0}(x)$ for some x, as well as code that solves the ODEs for $\eta(x)$ and $t(x)$. Another vital method is the one that yields the luminosity distance $d_L(x)$ for some x.

The specifics of our model was found from fits to (Planck Collaboration et al. 2021):

$$\begin{aligned} \text{Hubble constant:} &\quad h = 0.67 \\ \text{CMB temperature:} &\quad T_{\mathrm{CMB}0} = 2.7255\ \mathrm{K} \\ \text{effective Neutrino number:} &\quad N_{\mathrm{eff}} = 3.046 \\ \text{baryon density:} &\quad \Omega_{\mathrm{b}0} = 0.05 \\ \text{CDM density:} &\quad \Omega_{\mathrm{CDM}0} = 0.267 \\ \text{curvature density:} &\quad \Omega_{\mathrm{K}0} = 0 \end{aligned} \tag{17}$$

This gave the following derived parameters:

$$\begin{aligned} \text{photon density:} &\quad \Omega_{\gamma 0} = 5.51 \times 10^{-5} \\ \text{neutrino density:} &\quad \Omega_{\nu 0} = 3.81 \times 10^{-5} \\ \text{DE density:} &\quad \Omega_{\Lambda 0} = 0.683 \end{aligned} \tag{18}$$

We evaluated the various quantities over $x \in [-20, 5]$, the same interval for which we numerically solved the ODEs for $\eta(x)$ and $t(x)$ in Eq. (4), setting $x_{\mathrm{init}} = -20$ in Eq. (11).

After controlling our model by comparing numerical results to analytical expressions in limit cases, we turned our attention to the observational data from (Betoule et al. 2014). The data set is constructed as follows: for each redshift z_i, there is an observed luminosity distance $d_L^{\mathrm{obs}}(z_i)$ and an associated error $\sigma_{\mathrm{err}}(z_i)$.

Subsequently, we wrote a script to perform an MCMC for the parameters h, $\Omega_{\mathrm{m}0}$ and $\Omega_{\mathrm{K}0}$. Running said script, we compared the computed luminosity distance $d_L(z)$ from a cosmological model (an instance of the class) to the observed luminosity distance $d_L^{\mathrm{obs}}(z)$ through the χ^2-function,

$$\chi^2(h, \Omega_{\mathrm{m}0}, \Omega_{\mathrm{K}0}) = \sum_{i=1}^{N} \frac{\left(d_L(z_i; h, \Omega_{\mathrm{m}0}, \Omega_{\mathrm{K}0}) - d_L^{\mathrm{obs}}(z_i)\right)^2}{\sigma_{\mathrm{err}}^2(z_i)}, \tag{19}$$

where $N = 31$ is the number of data points. The best-fit model was considered as the one for which $\chi^2 = \chi^2_{\mathrm{min}}$, the lowest number found by the algorithm. A good fit is considered to have $\chi^2/N \sim 1$.

The MCMC analysis was characterised by a maximum of 10 000 iterations and the following limitations:

$$\begin{aligned} 0.5 \leq &\quad h \quad \leq 1.5 \\ 0.0 \leq &\quad \Omega_{\mathrm{m}0} \leq 1.0 \\ -1.0 \leq &\quad \Omega_{\mathrm{K}0} \leq 1.0 \end{aligned} \tag{20}$$

They were initialised by sample from a uniform distribution in the respective range. Once the code was executed successfully, we discard the first 200 samples, expecting this to be the approximate burn-in period for of the Metropolis MCMC.

2.3. Results

The familiar plot of the density parameters as functions of the logarithmic scale factor is presented in Fig. 1 together with markings of important milestones in the history of the universe (see Tab. 1).

The conformal Hubble factor and its derivatives are presented in Fig. 2 over-plotted with analytical predictions from the different eras (Tab. A.1). In the same figure you will find the product of the conformal time and Hubble factor.

The relationship between the cosmic and conformal time is demonstrated in Fig. 3, both quantities given in gigayears (“gigaannum” (Ga)).

We present the time of various milestones in the history of the universe, given this model, in Tab. 1 in our main time variable, redshift and cosmic time.

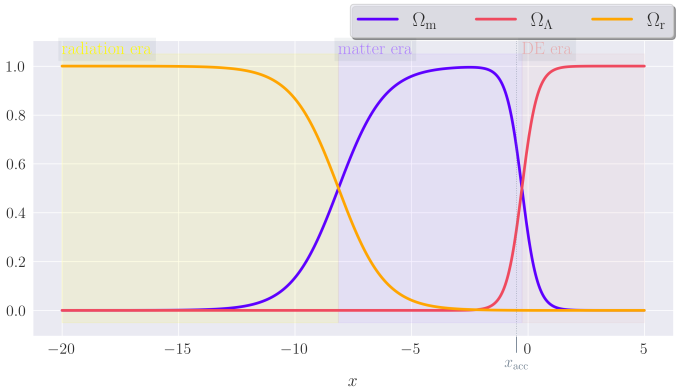

Fig. 1: The graphs show the evolution of the total matter density $\Omega_{\mathrm{m}}(x)$, the total radiation density $\Omega_{\mathrm{r}}(x)$ and the dark energy density $\Omega_\Lambda(x)$. The era of radiation ($x < x_{\mathrm{eq}}$), matter ($x_{\mathrm{eq}} < x < x_\Lambda$) and cosmological constant ($x > x_\Lambda$) domination are marked in yellow, purple and red, respectively.

Table 1: The values of the logarithmic scale factor x, the redshift z and the cosmic time t corresponding to four important milestones in the history of the universe.

	x	z	t
Rad.-matter equality	−8.132	3401	51.06 ka
Accel. begins	−0.4867	0.6270	7.753 Ga
Matter-DE equality	−0.2560	0.2918	10.37 Ga
Today	−0.000	0.000	13.86 Ga
Conformal time today:	$\eta_0 = 46.32c$ Ga		

2.3.1. Supernova fitting

Before adjusting any parameters, we compared our initial model with the supernova data from (Betoule et al. 2014). This by-eye comparison is found in Fig. 4.

The MCMC yielded $\chi^2_{\mathrm{min}} = 29.28$ for the best-fit. We present confidence regions for $\Omega_{\mathrm{m}0}$ and $\Omega_{\Lambda 0}$ in Fig. 5a at two levels; 68.4% and 95.5%. The distribution of the curvature parameter is shown in Fig. 5b. As for the Hubble constant, the distribution is found in Fig. 5c. The distributions were fitted as normal distributions (demonstrated in Fig. 5) $\mathcal{N}(\mu, \sigma)$ with average μ (best-fit) and standard deviation σ (error). We got the following set of new best-fits:

$$\begin{aligned} h &= 0.70 \pm 0.01 \\ \Omega_{\mathrm{m}0} &= 0.26 \pm 0.10 \\ \Omega_{\Lambda 0} &= 0.66 \pm 0.16 \\ \Omega_{\mathrm{K}0} &= 0.08 \pm 0.25 \end{aligned} \tag{21}$$

2.4. Discussion

The graphs in Fig. 1 show that prior to $x \sim -15$, radiation was the prevailing constituent of matter and energy density in the universe, making $x_{\mathrm{init}} = -20$ in Sec. 2.1.2 a valid choice. The radiation era is followed by an era of matter domination before the universe enters its current epoch where dark energy is the preeminent contributor to the cosmic energy budget. The universe has not yet become overwhelmed by the dark energy, however, and we can see that we are currently in a transitional period between total matter domination and total DE domination. The graphs also show that this transitional period is much quicker than the

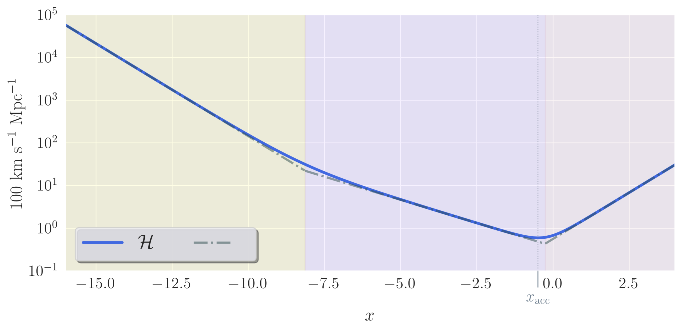

(a) The conformal Hubble factor $\mathcal{H}(x)$.

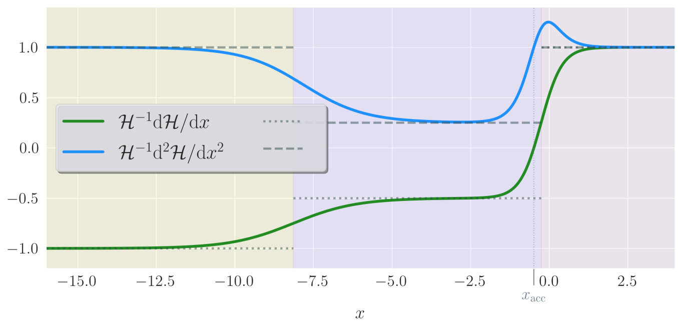

(b) The single and double derivative of the conformal Hubble factor, scaled with the factor itself, $\frac{1}{\mathcal{H}(x)}\frac{\mathrm{d}\mathcal{H}(x)}{\mathrm{d}x}$ and $\frac{1}{\mathcal{H}(x)}\frac{\mathrm{d}^2\mathcal{H}(x)}{\mathrm{d}x^2}$.

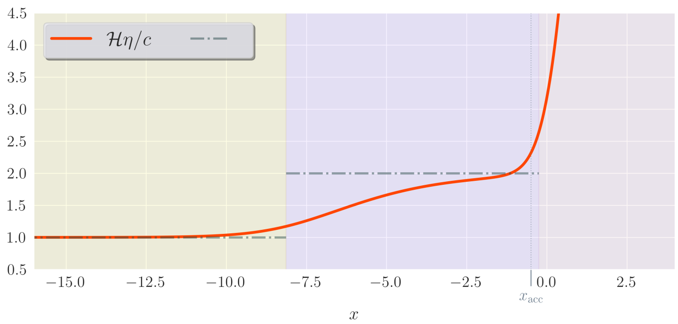

(c) The product of the conformal time and Hubble factor, divided by the speed of light, $\mathcal{H}(x)\frac{\eta(x)}{c}$. The solid graph blows up at late times.

Fig. 2: Plots demonstrating quantities related to the conformal Hubble parameter $\mathcal{H}(x)$ and the conformal time $\eta(x)$ as functions of logarithmic scale factor x. The dashed and/or dotted graphs are the predictions from Tab. A.1, i.e. what we expect in each era (indicated by different background colours, following Fig. 1) if all non-prevailing constituents can be neglected. The beginning of acceleration is indicated by a humble vertical line.

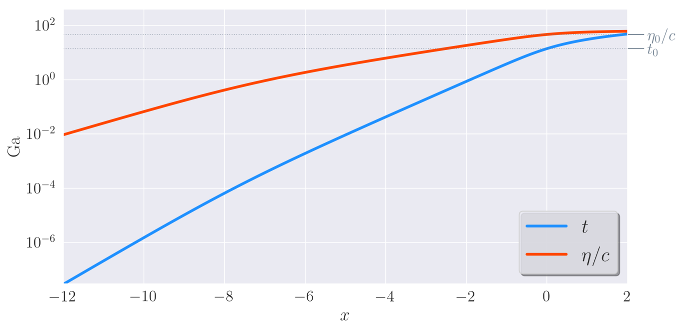

Fig. 3: Cosmic time $t(x)$ and conformal time per speed of light $\frac{\eta(x)}{c}$.

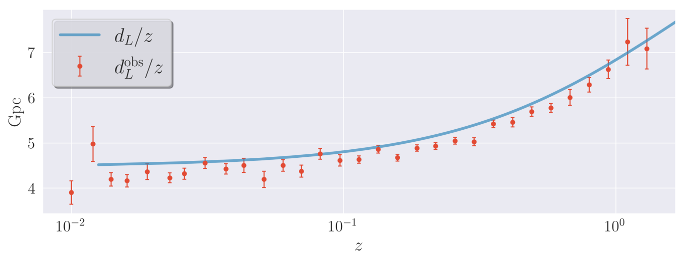

Fig. 4: The observed and computed luminosity distance per redshift $\frac{d_L^{\mathrm{obs}}(z)\pm\sigma_{\mathrm{err}}(z)}{z}$ and $\frac{d_L(z)}{z}$.

previous one, and that just before matter-DE equality ($x = x_\Lambda$), the universe starts accelerating ($x = x_{\mathrm{acc}}$). We clearly see the relation between the dark energy suddenly becoming significant and the universe accelerating.

Our results, as shown in the graphs in Fig. 2, demonstrate that our code gives sensible results when modelling the evolution of the universe. The changes in the density parameters depicted in Fig. 1 offer insight into the transitional periods shown in Fig. 2a and Fig. 2b, which correspond to eras where no single substance dominates the universe. These findings are consistent with existing knowledge of the universe's history. Additionally, we observe that the conformal time cannot be accurately predicted in the same way for later eras, as demonstrated in Fig. 2c, exactly as expected (ref to some section).

In this model, the redshift of 3400 marks the epoch of radiation-matter equality, while the universe entered its current epoch approximately 3.5 gigayears ago as shown in Tab. 1. Additionally, our analysis reveals that the universe is estimated to be 13.9 gigayears old and has been accelerating for almost half of that time, starting at the age of 7.8 gigayears. These predictions differ slightly from those reported in the literature, such as an age of $t_0 = 13.78$ in (Dodelson & Schmidt 2021). It is sufficient to argue that the main reason for such deviations is the (small) difference in choice of cosmological parameters. However, we would like to address the computational limitations: the choice of grid for x may introduce numerical vulnerabilities that propagate into other variables. For instance, as illustrated in Fig. 3, over 10 gigayears can pass between $x = -2$ and $x = 0$, even though we started integrating from $x = x_{\mathrm{init}} = -20$.

2.4.1. Supernova fitting

The comparison of our model's luminosity distance with observational data, as shown in Fig. 4, suggests that our model could benefit from some adjustments. While the deviations are not too far off, it is clear that there is some room for improvement. However, it is important to note that the discrepancies may not be solely due to the three parameters we chose to study.

To further constrain our model, we performed an MCMC analysis and examined the resulting distributions of parameters. The scatter plot in Fig. 5a shows that our model requires an accelerating universe ($\mathrm{d}\mathcal{H}/\mathrm{d}x\,|_{x=x_0} > 0$) with a strictly positive cosmological constant ($\Omega_{\Lambda 0} > 0$). We notice that the Planck parameters lie within the 1σ region for ($\Omega_{\mathrm{m}0}$, $\Omega_{\Lambda 0}$), along the flat line. This is not the case for all the parameters, however.

Interestingly, the data clearly prefer a slightly higher value for the little Hubble parameter h than our fiducial value of 0.67, as shown in the narrow histogram in Fig. 5c. The PDFs of the density parameters $\Omega_{\mathrm{m}0}$ and $\Omega_{\Lambda 0}$ are much broader, but the algorithm manages to narrow the possibilities down significantly.

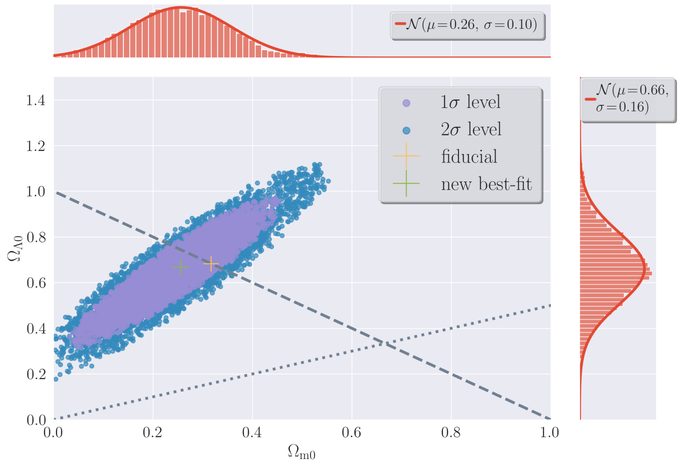

(a) The dots give constraints on the parameters that quantify the contribution of matter and cosmological constant to the cosmic energy budget today (Ω_{m0}, $\Omega_{\Lambda 0}$). The Planck parameters from Eq. (17) and Eq. (18) and the new best-fit parameters are indicated by crosses. The dashed grey line points to a flat universe; below/above this meaning an open/closed universe. The dotted grey line signifies zero acceleration; below/above indicating a decelerating/accelerating universe. The distributions of the accepted samples of Ω_{m0} and $\Omega_{\Lambda 0}$ are illustrated by the top and right panel, respectively.

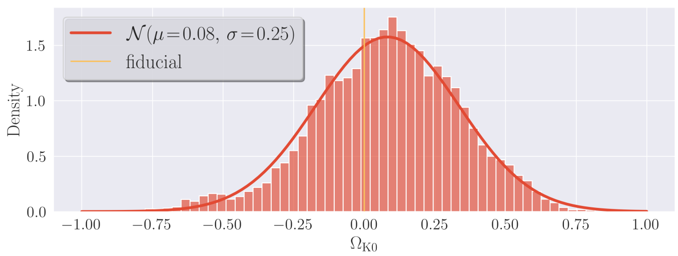

(b) Posterior distribution of parameter quantifying the contribution of curvature to the cosmic energy budget today.

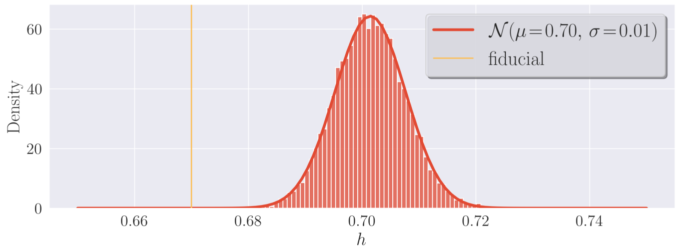

(c) Posterior distribution of the Hubble constant $h = H_0$ [100 km s^{-1} Mpc^{-1}].

Fig. 5: Results from the MCMC of 10 000 iterations. The histograms show the distributions of accepted samples and the curves are their PDFs.

One potential concern is the uncertainty in the curvature parameter Ω_{K0}, as shown in Fig. 5. The data seem to favour a negatively curved universe, but the allowed range is quite broad. This may indicate that our model needs further refinement to better account for the effects of curvature.

Overall, our primitive MCMC analysis provides valuable insights into the constraints on the parameters of our model and highlights areas where further improvements could be made. Other than with observational data from supernovae, there are several ways of constraining the cosmological parameters, such as measuring the CMB anisotropies. The Planck Collaboration (Planck Collaboration et al. 2021) provides a set of cosmological parameters that are significantly more solid, in the sense that their results are tested and compared thoroughly. This is why we proceed using the fiducials from Eq. (17) and Eq. (18).

3. Recombination history

REPHRASE: Following the Big Bang (BB), the universe was very hot and dense. Under such extreme conditions, atoms cannot exist. Before atoms formed in the universe, all matter was distributed as a highly ionised plasma. As the universe expanded, the density and temperature decreased. Eventually, the conditions allowed for *recombination* of ions and electrons. That is, atoms (vastly H and He) formed during the "epoch of recombination" approximately 380 000 years after BB, at which the temperature had dropped to ~ 3000 K. Prior to this, the photons were by no means able to travel freely through the ionised plasma as they interacted with free electrons through Thomson scattering. As the free electrons paired up with other baryons to form neutral atoms during recombination, the mean free path (MFP) of the photons increased. The photons emitted at this point in time is what makes up the CMB.

We will in this section examine the free electron fraction and followingly the optical depth and visibility function.

3.1. Theory

Photons travelling through a medium may be absorbed. The intensity of light emitted from a distance x is reduced by the factor $e^{-\tau(x)}$ where $\tau(x)$ is the optical depth of the medium. In cosmology, Thomson scattering ($\gamma + e^- \leftrightarrows \gamma + e^-$) is predominantly responsible for the absorption of photons universe, and we find the optical depth through the ODE in x

$$\frac{\mathrm{d}\tau}{\mathrm{d}x} = -\frac{n_e \sigma_\mathrm{T} \mathrm{e}^x}{\mathcal{H}(x)}, \tag{22}$$

where σ_T is the Thomson scattering cross-section and n_e the electron density. A related quantity is the visibility function

$$\tilde{g}(x) = -\mathrm{e}^{-\tau(x)} \frac{\mathrm{d}\tau}{\mathrm{d}x}, \tag{23}$$

a proper probability distribution since we demand $\int_{-\infty}^{0} \mathrm{d}x\, \tilde{g}(x) = 1$.

3.1.1. Saha approximation

Consider the interaction that keeps electrons (e^-) and protons (p^+) in equilibrium with photons (γ),

$$e^- + p^+ \leftrightarrows \mathrm{H} + \gamma. \tag{24}$$

We define the fractional electron density $X_e \equiv n_e/n_\mathrm{b}$ where $n_\mathrm{b} \approx n_p + n_\mathrm{H} = n_e + n_\mathrm{H}$ is the total baryon number density.

$$n_\mathrm{H} = (1 - Y_P)\, n_\mathrm{b} \simeq \frac{\Omega_{\mathrm{b}0}\rho_{\mathrm{cr}0}}{m_\mathrm{H} \mathrm{e}^{3x}} \tag{25}$$

$$\frac{X_e^2}{1 - X_e} = \frac{1}{n_\mathrm{b}} \left(\frac{m_e T_\mathrm{b}}{2\pi}\right)^{3/2} \mathrm{e}^{-B_1/k_b T_\mathrm{b}} \tag{26}$$

3.1.2. Peebles equation

$$\frac{\mathrm{d}X_e}{\mathrm{d}x} = \frac{C_r(T_\mathrm{b})}{\mathcal{H}(x)\mathrm{e}^{-x}} \left[\beta(T_\mathrm{b})\,(1 - X_e) - n_\mathrm{H}\alpha^{(2)}(T_\mathrm{b}) X_e^2\right] \tag{27}$$

$$C_r(T_\mathrm{b}) = \frac{\Lambda_{2s\to1s} + \Lambda_\alpha}{\Lambda_{2s\to1s} + \Lambda_\alpha + \beta^{(2)}(T_\mathrm{b})} \tag{28a}$$

$$\beta(T_\mathrm{b}) = \left(\frac{m_e k_\mathrm{B} T_\mathrm{b}}{2\pi\hbar^2}\right)^{3/2} \mathrm{e}^{-B_1/k_b T_\mathrm{b}} \alpha^{(2)}(T_\mathrm{b}) \tag{28b}$$

$$\alpha^{(2)}(T_\mathrm{b}) = \frac{64\pi}{\sqrt{27\pi}} \frac{e^4}{m_e^2 c^3} \sqrt{\frac{B_1}{k_b T_\mathrm{b}}} \phi_2(T_\mathrm{b}) \tag{28c}$$

$$\beta^{(2)}(T_\mathrm{b}) = \beta(T_\mathrm{b}) \mathrm{e}^{3B_1/4k_b T_\mathrm{b}} \tag{28d}$$

3.2. Implementation details

3.3. Results

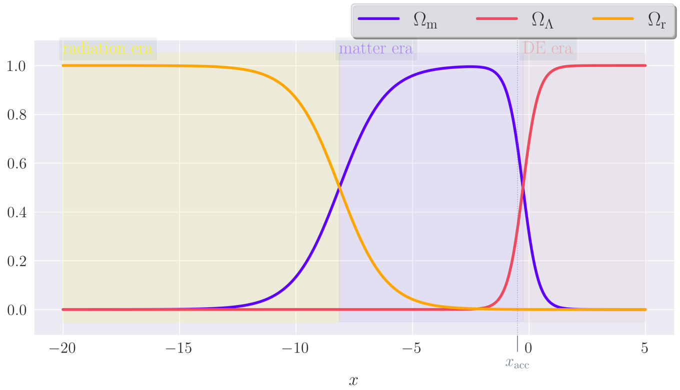

Fig. 6: The fractional electron density $X_e(x)$ resulting from the Peebles and Saha equations.

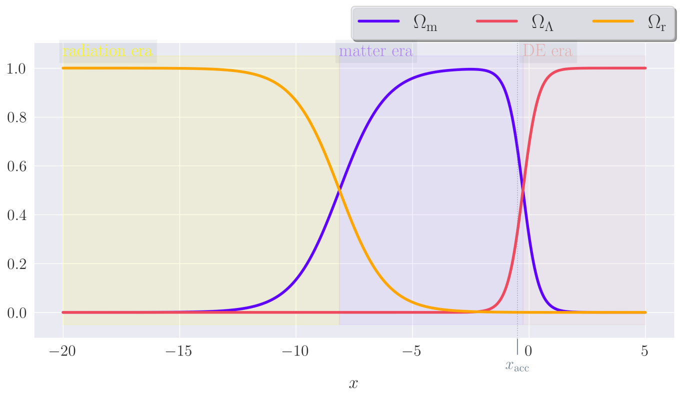

Fig. 7: The optical depth $\tau(x)$ and its derivatives $-\frac{\mathrm{d}\tau(x)}{\mathrm{d}x}$ and $\frac{\mathrm{d}^2\tau(x)}{\mathrm{d}x^2}$ as functions of logarithmic scale factor x.

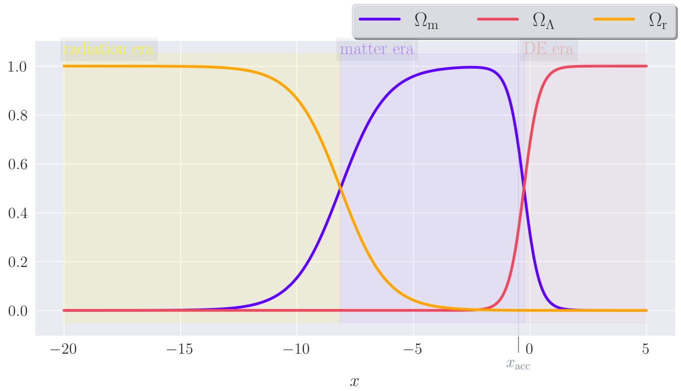

Fig. 8: The visibility function $\tilde{g}(x)$ and its derivatives $\frac{\mathrm{d}\tilde{g}(x)}{\mathrm{d}x}$ and $\frac{\mathrm{d}^2\tilde{g}(x)}{\mathrm{d}x^2}$ as functions of logarithmic scale factor x.

3.4. Discussion

4. Conclusion

References

Betoule, M., Kessler, R., Guy, J., et al. 2014, A&A, 568, A22
Callin, P. 2006, arXiv e-prints, astro
Dodelson, S. & Schmidt, F. 2021, Modern Cosmology, 2nd edn.
Planck Collaboration, Aghanim, N., Akrami, Y., et al. 2021, A&A, 652, C4

Appendix A: Conformal Hubble parameter

Revisit the general form of the first Friedmann equation from Sec. 2.1.2, i.e.

$$\mathcal{H}(x) = H_0 \sqrt{\sum_s \Omega_{s0} e^{-(1+3w_s)x}}, \tag{A.1}$$

where sum over s is a sum over the constituents in the universe ($s \in \{\mathrm{m}, \mathrm{r}, \Lambda, \mathrm{K}\}$) and w_s represents the species' equation of state parameter. As a shorthand notation, we introduce $\Xi_m = \Xi_m(x)$ given by

$$\Xi_m(x) \equiv \sum_s (-1)^m (1+3w_s)^m \Omega_{s0} e^{-(1+3w_s)x}; \quad m \in \mathbb{N}, \tag{A.2}$$

s.t. $\mathrm{d}^n X_m/\mathrm{d}x^n = \Xi_{m+n}$. Now $\mathcal{H} = H_0 \sqrt{\Xi_0}$ and its first derivative becomes

$$\frac{\mathrm{d}\mathcal{H}}{\mathrm{d}x} = H_0 \frac{\Xi_1}{2\sqrt{\Xi_0}}. \tag{A.3}$$

The second derivative is obtained through the quotient rule, i.e.

$$\begin{aligned}\frac{\mathrm{d}^2\mathcal{H}}{\mathrm{d}x^2} &= \frac{H_0}{2} \frac{\Xi_2 \sqrt{\Xi_0} - \Xi_1 \frac{\Xi_1}{2\sqrt{\Xi_0}}}{\Xi_0} \\ &= H_0 \frac{\Xi_1}{2\sqrt{\Xi_0}} \left(\frac{\Xi_2}{\Xi_1} - \frac{\Xi_1}{2\Xi_0} \right).\end{aligned} \tag{A.4}$$

Now that we have these expressions, let us look at some special cases. Assume that the universe only consists of the substance s. Then

$$\Xi_m = (-1)^m (1+3w_s)^m \Omega_{s0} e^{-(1+3w_s)x}. \tag{A.5}$$

We obtain the following:

$$\frac{1}{\mathcal{H}}\frac{\mathrm{d}\mathcal{H}}{\mathrm{d}x} = \frac{\Xi_1}{2\Xi_0} \qquad = -\frac{1}{2}(1+3w_s) \tag{A.6a}$$

$$\frac{1}{\mathcal{H}}\frac{\mathrm{d}^2\mathcal{H}}{\mathrm{d}x^2} = \frac{\Xi_1}{2\Xi_0}\left(\frac{\Xi_2}{\Xi_1} - \frac{\Xi_1}{2\Xi_0} \right) \qquad = +\frac{3}{4}(1+3w_s)^2 \tag{A.6b}$$

As for the conformal time, we get an expression that is ill-defined for some cases:

$$\begin{aligned}\frac{\eta\mathcal{H}}{c} &= \mathcal{H} \int_{-\infty}^{x} \mathrm{d}x' \, \frac{1}{\mathcal{H}} \\ &= e^{\frac{x}{2}(1+3w_s)} \int_{-\infty}^{x} \mathrm{d}x' \, e^{-\frac{x'}{2}(1+3w_s)} \\ &= \begin{cases} \frac{2}{1+3w_s} & w_s > {}^1\!/_3 \\ \infty & w_s \leq -{}^1\!/_3 \end{cases}\end{aligned} \tag{A.7}$$

We have gathered a set of analytical predictions for different eras in the history of the universe. The detailed result is presented in Tab. A.1. Note, however, that to compare this last expression to the numerical result does not actually make sense for later times as $\eta(x)$ depends on the historic composition as well.

Table A.1: Analytical predictions for single-substance universes.

	w_s	$\mathcal{H}/H_0$	$\frac{1}{\mathcal{H}}\frac{\mathrm{d}\mathcal{H}}{\mathrm{d}x}$	$\frac{1}{\mathcal{H}}\frac{\mathrm{d}^2\mathcal{H}}{\mathrm{d}x^2}$	$\frac{\eta\mathcal{H}}{c}$
Radiation-dominated	$^1/_3$	$\sqrt{\Omega_{\mathrm{r}0}}e^{-x}$	-1	1	1
Matter-dominated	0	$\sqrt{\Omega_{\mathrm{m}0}}e^{-^1/_2 x}$	$-^1/_2$	$^1/_4$	2
DE-dominated	-1	$\sqrt{\Omega_{\Lambda0}}e^{x}$	1	1	∞